Meteoritics & Planetary Science 42, Nr 4/5, 801–809 (2007)
Abstract available online at http://meteoritics.org

Physical property measurements: ICDP boreholes LB-07A and LB-08A, Lake Bosumtwi impact structure, Ghana

William A. MORRIS, Hernan UGALDE,* and Christina CLARK

McMaster Applied Geophysics and Geological Imaging Consortium, School of Geography & Earth Sciences, McMaster University, 1280 Main Street West, Hamilton, Ontario, L8S 4K1, Canada
*Corresponding author. E-mail: ugaldeh@mcmaster.ca

(Received 26 July 2006; revision accepted 12 January 2007)

Abstract–Physical rock property measurements provide the primary constraints for any geological models hypothesized from geophysical observations. Previous geophysical models of the Bosumtwi impact structure hypothesized that a highly magnetic and dense impact-melt sheet might be the source of the observed magnetic anomalies. However, magnetic susceptibility and density measurements made on International Continental Scientific Drilling Program (ICDP) cores LB-07A and LB-08A from the interior of the Bosumtwi meteorite impact structure contain no evidence for that. Both density and magnetic susceptibility logs on both boreholes exhibit low-amplitude contrasts between the uppermost polymict lithic breccia and suevite, the intermediate monomict lithic breccia, and the lowermost bedrock. The depth extent of fracture-related density reduction is much greater at LB-08A than at LB-07A. A total magnetic intensity log from borehole LB-08A supports the suggestion that magnetic anomalies over Lake Bosumtwi are mainly sourced in undetected and/or covered bedrock intrusions, like the ones outcropping at the northeast and to the southwest of the lake.

INTRODUCTION

The detailed morphology of the Bosumtwi structure, Ghana (located at 6.5°N, 1.4°W), like at many other meteorite impact sites, is mostly hidden by the water of the crater lake and its associated sediments (e.g., Clearwater East and West, Dence et al. 1965; Wanapitei, Dence and Popelar 1972). Commonly in such a case, the hidden subsurface structure is interpreted from geophysical data. Plado et al. (2000), for example, hypothesized that the observed magnetic anomaly over Lake Bosumtwi can be explained by "one or several relatively strongly remanently magnetized impact-melt rock or melt-rich suevite bodies." All geological models calculated from geophysical data are non-unique. Antipathetically varying physical contrast and depth of the source body over a range of values can produce geophysical responses that are indistinguishable (Hearst and Morris 1995). In this type of situation, additional external constraints are needed in order to determine which model is most geologically viable. There are two possible sources for this additional information: a) physical rock property data from the actual study area, and/or b) borehole geophysical data that can provide constraints on the depth distribution of anomalous source bodies. While Plado et al. (2000) had access to some limited magnetic property data from samples collected around Lake Bosumtwi, they argued that the magnetization of these samples had been diminished by weathering and alteration processes and thus they were not representative of the real magnetization parameters of the impact-melt rocks under the lake. To support their model, Plado et al. (2000) required strongly magnetic material in the form of impact melt. In contrast, Ugalde et al. (2007b) have proposed that the observed magnetic anomaly can be explained by weakly magnetic layers of impactite material overlying the crater floor, with the larger magnetic anomalies being attributed to granites and other intrusives in the Proterozoic basement.

To determine which of these opposing models is most viable requires additional rock property and borehole information. Subsequent to the original model work of Plado et al. (2000), two deep International Continental Scientific Drilling Program (ICDP) boreholes were drilled into the Bosumtwi impact structure. The location of these boreholes (LB-07A and LB-08A) is not coincident with the location of any of the magnetic anomalies (Fig. 1) (Ugalde et al. 2007b). Seismic profile evidence suggests that LB-07A extends into the crater floor below the crater moat surrounding the small central uplift, whereas LB-08A is into the flank of the central uplift (Fig. 2).

This paper reports both physical property data and borehole log information. Density and magnetic susceptibility

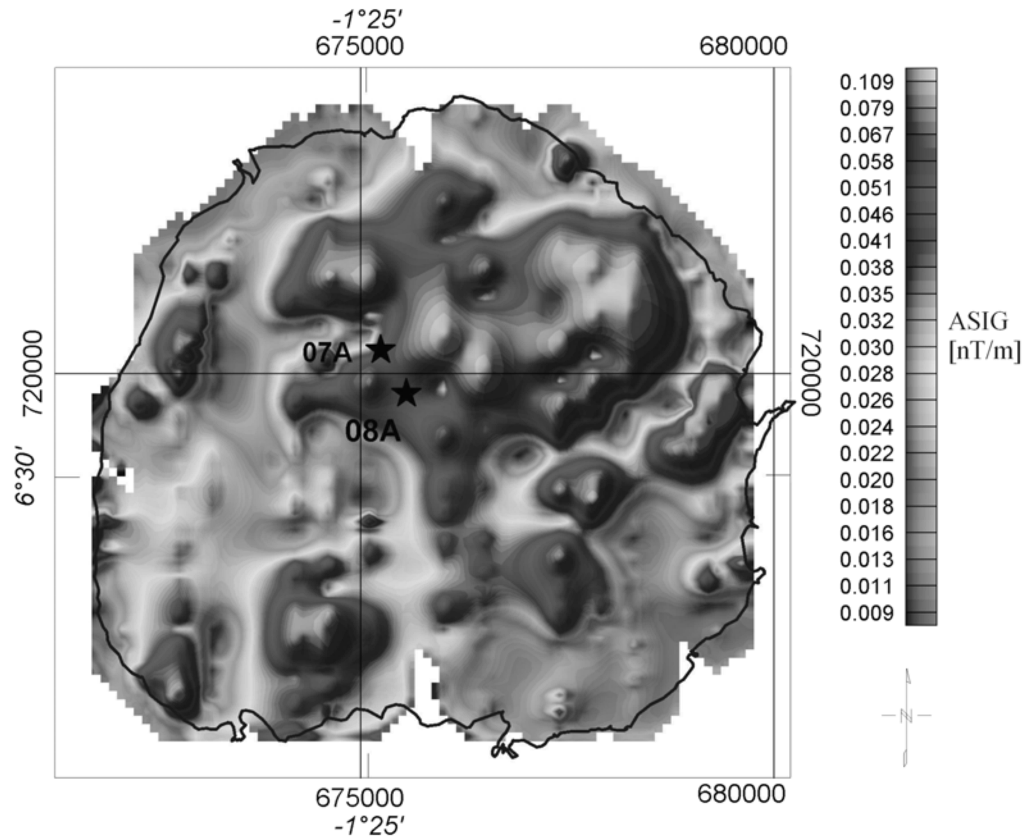

Fig. 1. Amplitude of the analytical signal from the observed total magnetic field. This transformation is computed as the square root of the sum of the gradients of the total field, squared:

$$[A(x,y)] = \sqrt{\left(\frac{\partial T}{\partial x}\right)^2 + \left(\frac{\partial T}{\partial y}\right)^2 + \left(\frac{\partial T}{\partial z}\right)^2}$$

where $A(x,y)$ is the analytical signal (ASIG) and T is the total magnetic field, and its maxima are centered over the magnetic sources (see Ugalde et al. 2007b for details). The locations of boreholes LB-07A and LB-08A are marked in black. Marine magnetic data from Danuor (2004).

measurements were made on core material at the ICDP facilities of the GeoForschungsZentrum (GFZ) in Potsdam, Germany, in 2004 (Milkereit et al. 2006; Ugalde 2006). Borehole total magnetic field data were extracted from the borehole deviation surveys performed by ICDP staff in both boreholes.

PREVIOUS PHYSICAL PROPERTY MEASUREMENTS AT BOSUMTWI

Meteorite impacts can greatly modify the magnetic properties of the target rocks, either enhancing them (higher magnetic susceptibility because of shock decomposition of original minerals into more magnetic facies [Chao 1968; Henkel and Reimold 2002; Ugalde et al. 2005]), or reducing them (magnetic susceptibility reduction at $P > 10$ GPa due to modification of magnetic carriers due to the high impact-related pressures [Pilkington and Grieve 1992]; shock demagnetization at $P < 1$ GPa [Cisowski and Fuller 1978]).

At the Bosumtwi structure, Plado et al. (2000) demonstrated that there is a clear difference between petrophysical properties of the target rocks and the impact-derived suevites. Suevites sampled around the lake have low densities (higher porosities) and somewhat higher magnetizations (susceptibility, remanent magnetization) compared to the target (country) rocks (Plado et al. 2000). The remanent magnetization of suevites prevails over their induced magnetization. The Koenigsberger ratio of remanent over induced magnetization is much higher than 1:

$$Q = \frac{\|\overline{M}_R\|}{\|\overline{M}_1\|} \sim 4 \qquad (2)$$

The target rocks have strikingly homogeneous physical properties with noticeable weak remanent magnetization and Q values ($Q < 0.05$). A graphite shale sampled by Plado et al. (2000) shows fairly high remanent magnetization, whereas the granites (like the Pepiakese body) are magnetically very

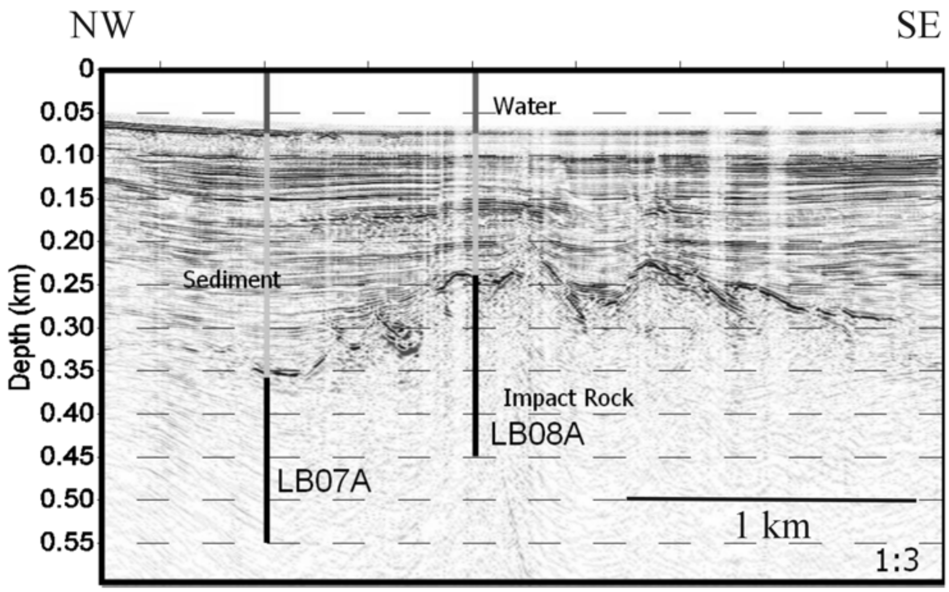

Fig. 2. The depth extent of boreholes LB-07A and LB-08A relative to the observed basal morphology of the Bosumtwi impact crater as imaged by seismic reflection survey. Note the 1:3 vertical exaggeration. Modified from Scholz et al. (2002).

weak (Plado et al. 2000). Unfortunately, there are no measurements on magnetic properties on the Kumasi batholith to the north of the lake, and the Bansu intrusion to the southwest, as both of them exhibit a direct spatial correlation with the airborne magnetic anomalies (Ugalde et al. 2007b).

Natural remanent magnetization (NRM) was measured in a few selected samples in both boreholes (Elbra et al. 2007; Kontny et al. 2007). In general, NRM intensities on impact breccias vary between 0.4 and 200 mA/m, with largest values up to 100 A/m (Kontny et al. 2007). Although these values are higher than the NRM intensities reported for the country rocks sampled around the lake (0.1–39 mA/m) (Plado et al. 2000), pre-impact pyrrhotite was remagnetized by the impact (Kontny et al. 2007). However, it does not occur in sufficiently large volumes (mostly below 1% volume) (Kontny et al. 2007) to have a noticeable effect on the measured total field and thus could not account for the large magnetic anomalies observed on the lake (Ugalde et al. 2007b).

NEW PHYSICAL PROPERTY MEASUREMENTS

Magnetic Susceptibility

Magnetic susceptibility measurements were collected at ~10 cm intervals on all the core pieces that were suitable for this purpose, that is, pieces that were not broken and where flat surfaces were available to carry out the measurement. Each measurement was made with a Bartington MS-2 meter with an E probe attachment. The volume of all samples (70 mm diameter core) was much greater than the size of the detector, which had a 3.8 × 10.5 mm area of response. Repeat calibration measurements were made against a known standard. Hole LB-07A exhibits moderately low susceptibilities over most of its length (Fig. 3). In more detail, the susceptibility data represent three groupings that are directly equivalent to the lithological log (Coney et al. 2007). The lowermost section (>470 m depth) comprises meta-graywacke, shale, slate, and schist of the basement and has the highest overall magnetic susceptibility values of 35–50 × 10^{-5} SI. The next block which corresponds to the monomict breccia zone (415–470 m) has the lowest magnetic susceptibility with values less than 20 × 10^{-5} SI. The uppermost zone (360–410 m depth) of polymict lithic impact breccia and suevite has intermediate magnetic susceptibility values between those found in the other two zones. Each of the boundaries between the three zones is defined by a sharp sudden decrease and a sharp increase in susceptibility values. Locally, some units (uppermost polymict lithic breccia and the lowermost suevite within the uppermost interval) appear to have internal susceptibility structure, an equivalent for which has not been observed in the lithostratigraphy. However, due to the sampling resolution of the surface magnetic sensors, for the purposes of any magnetic modeling exercise the stratigraphic column is best represented by a simple three-layer model.

Hole LB-08A can be divided into 4 zones: low magnetic susceptibility, from 240 to 270 m depth, with values around 10–15 × 10^{-5} SI (polymict lithic breccia and graywacke) (Ferrière et al. 2007; Koeberl et al. 2007); moderate magnetic susceptibilities, from a depth of 270 to 315 m and then to a depth of 370 to 425 m, with values around 40 × 10^{-5} SI (graywacke, shale, slate, phyllite, schist and narrow suevite

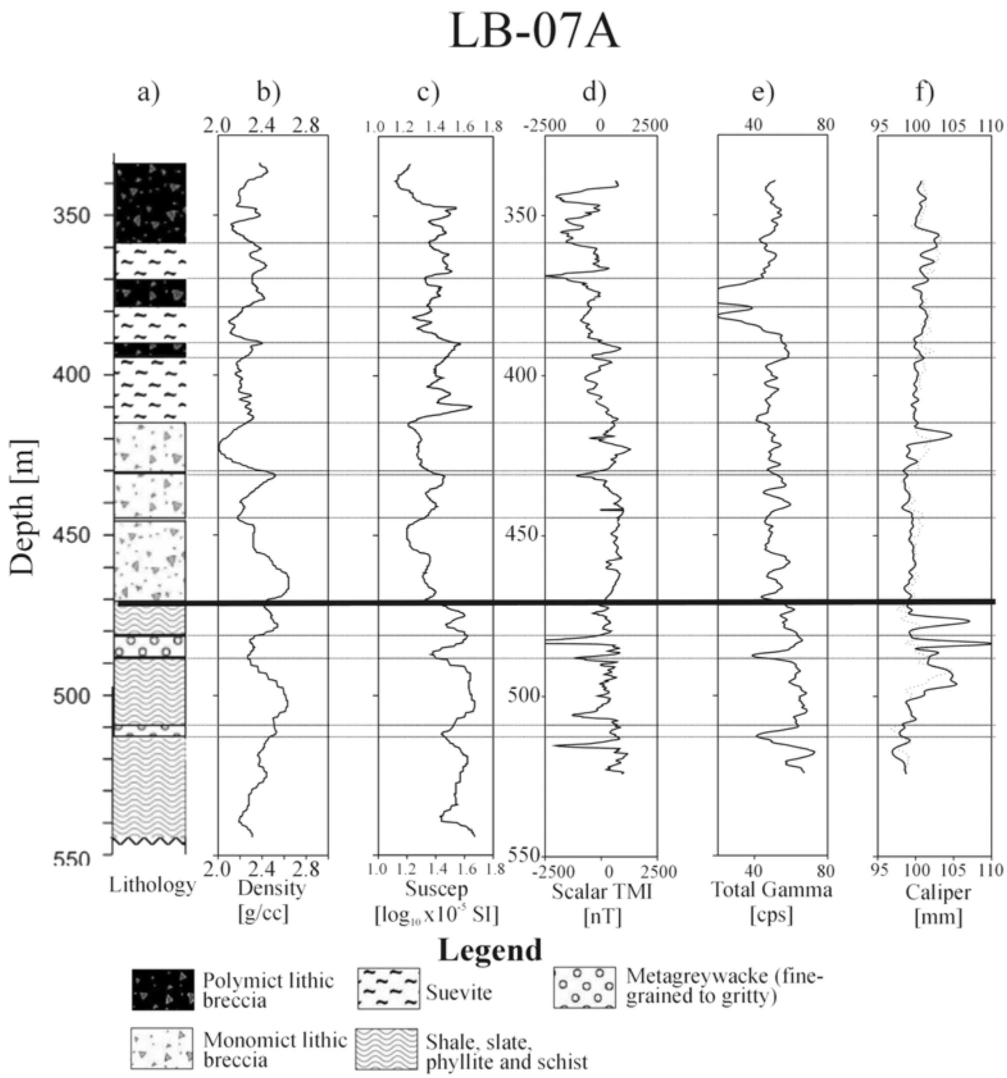

Fig. 3. Physical property logs for borehole LB-07A. Individual logs are (a) simplified lithology modified from Koeberl et al. (2007) (compare Coney et al. 2007); (b) density (g/cm^3) measured on core segments; (c) magnetic susceptibility ($\log_{10} \times 10^{-5}$ SI) measured on core segments; (d) TMI (nT), scalar magnetic intensity derived from borehole deviation survey; (e) total gamma derived from borehole survey by ICDP (cps); and (f) caliper (mm) survey derived from borehole survey by ICDP. The thick black line marks the crater floor.

dikes) (Ferrière et al. 2007); high magnetic susceptibilities, from a depth of 315 to 370 m, with values around 50–70 × 10^{-5} SI (graywacke, shale, slate, phyllite, schist) (Ferrière et al. 2007) also exhibiting 10 m wide intervals of enhanced susceptibilities (Fig. 4). The shale/slate/schist unit locally exhibits a higher magnetic susceptibility than the graywacke units.

Density

Density measurements were collected at the ICDP facilities at GFZ using their gamma-ray attenuation density estimation facility. Rock density is calculated from a count of the gamma flux detected on the opposite side of the test sample from the reference gamma source. The calculated density is affected by the overall diameter and length of the core sample. To avoid inconsistencies in the results, it was necessary to ensure that only those samples that were uniformly cylindrical with a diameter of 70 mm were measured. The densities of a number of core samples were initially measured using a water-immersion technique. As noted by Elbra and Pesonen (2006), the water-immersion densities are systematically higher than the gamma-density values. The differences might be related to minor variations in the diameter of the core pieces used for the gamma-ray attenuation density measurements, which would yield to some calibration variations. Still, this difference is insufficient to have any impact on any modeling done on the gravity data.

Density values in LB-07A exhibit the same threefold

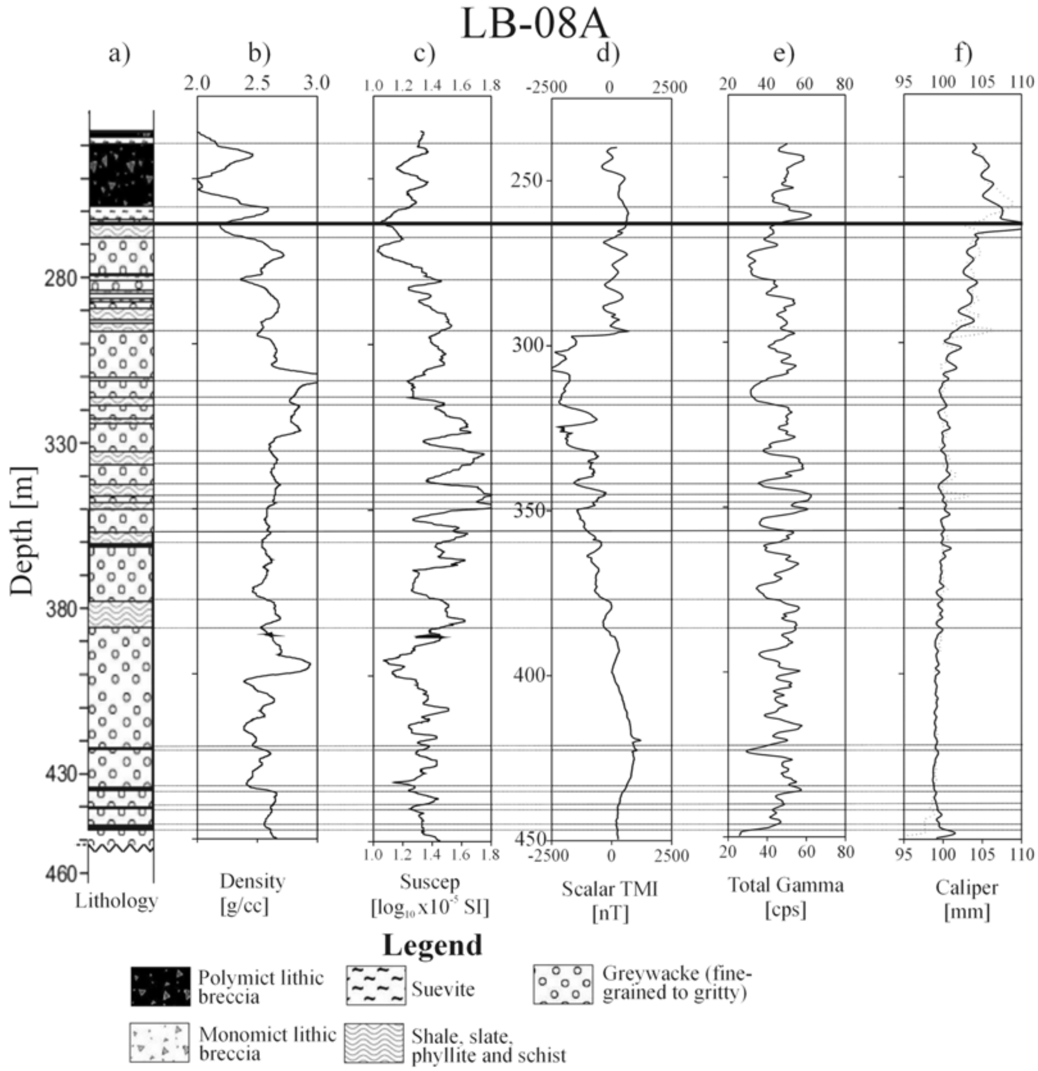

Fig. 4. Physical property logs for borehole LB-08A. Individual logs are (a) simplified lithology modified from Koeberl et al. (2007); (compare Ferrière et al. 2007); (b) density (g/cm^3) measured on core segments; (c) magnetic susceptibility ($\log_{10} \times 10^{-5}$ SI) measured on core segments; (d) TMI (nT), scalar magnetic intensity derived from borehole deviation survey; (e) total gamma derived from borehole survey by ICDP (cps); and (f) caliper (mm) survey derived from borehole survey by ICDP. The thick black line marks the crater base.

subdivision as noted for susceptibility measurements: the uppermost polymict lithic impact breccia and suevite have the lowest density averaging around 2.25 g/cm^3, the monomict breccia has slightly higher density of around 2.36 g/cm^3, and the basement has a density around 2.40 g/cm^3. One noticeable feature is the low density zone at the top of the monomict breccia unit (Fig. 3). Density values in LB-08A systematically increase with increasing depth from 240 m to around 310 m, with values from less than 2.0 g/cm^3 in the polymict impact breccia to around 2.5 g/cm^3 in the basement (Fig. 4). Below 310 m, the density is fairly uniform and greater than 2.5 g/cm^3. A zone with a density lower than 2.4 g/cm^3 exists within the graywacke unit from 400 to 435 m.

For the purposes of gravity modeling, the geological structure was modeled using a simple four-layer model comprising water, sediments, impactites, and basement (see Ugalde et al. 2007a). Lateral differences in the density of the basement rocks between boreholes LB-07A and LB-08A, which must be incorporated into any gravity model, are probably related to the fact that LB-08A is on the central uplift. As discussed by Ugalde et al. (2007a), the lateral variations on maximum pressure reached by the impact have an effect on the porosity distribution throughout the crater, and thus on its spatial density variations.

Total Gamma Radiation

A total gamma radiation borehole survey was completed in each of the two boreholes. Both logs exhibit oscillations possibly related to localized lithological variations. Borehole

LB-07A, for example, shows a marked decrease in total gamma response associated with the second polymict lithic impact breccia horizon. Neither of the two holes contains any evidence for the zone of enhanced gamma response around the impact structure that has been mapped using airborne geophysics (Fig. 22 of Pesonen et al. 2003). To investigate the observed potassium concentration, Boamah and Koeberl (2003) carried out an extensive chemical analysis of 54 soil samples from around the Bosumtwi impact structure. Soils from the area having a high radiometric potassium signal do have higher potassium content. Boamah and Koeberl (2003) then suggested that this might reflect potassium mobilization produced as a consequence of the impact event. This does not agree with the evidence reported from the borehole logs. Plotting the airborne radiogenic potassium signal on the topographic signal shows that there is a very close association between the two responses (see Figs. 6 and 13 of Koeberl and Reimold 2005). The genesis of this association therefore remains unexplained.

Total Magnetic Intensity

Borehole total magnetic intensity (TMI) surveys are not common in exploration geophysics. However, borehole deviation probes normally include and make use of magnetometers to measure the attitude of the borehole. All borehole deviation surveys are the result of two data sets: a) measurement of the local dip of the borehole, and b) measurement of dip direction relative to some absolute reference frame. Many borehole probes use Earth's magnetic field direction for external reference. The orientation of the magnetic direction is calculated from a suite of tri-axial fluxgate magnetometers. For borehole navigation purposes, the probe orientation is calculated from the ratio of the two subhorizontal magnetic sensors. Together the three fluxgate sensors provide a measure of the variation of total magnetic field intensity versus depth in the borehole.

For this study we reprocessed the borehole deviation data to provide TMI logs for boreholes LB-07A and LB-08A (Figs. 3 and 4). Data corrections done included: between sensor gain and offset adjustments, between sensor nonorthogonality corrections, and individual sensor drift corrections. Regional/residual separation was accomplished by computing the difference between the average TMI value for each borehole and the value at each observation point. No diurnal field correction was applied as correction data were not available. However, the range of the borehole TMI data collected (10^3 nT) is beyond the expected diurnal variation of the magnetic field at the lake surface (10^1 nT).

A borehole TMI survey records the response of all magnetic sources within the detection range. Like standard airborne and ground magnetic surveys, TMI is the vector summation of both induced and remanent magnetic field contributions. There are two very important differences between borehole and surface TMI surveys. First, in a borehole survey the source-sensor separation is very small. In most cases the distance between the probe and the surrounding wall of the drill hole is much less than one centimeter. In contrast, for all surface or airborne TMI surveys the source-sensor distance is more commonly tens to hundreds of meters. Both the signal amplitude and frequency response of a borehole TMI survey will always be much higher than for a surface survey. Second, a borehole may have two types of source-sensor configuration: a) an on-hole magnetic source where the borehole passes through the magnetic body, and b) an off-hole magnetic source where the borehole does not intersect the magnetic source. The off-hole configuration is similar to the type of situation one normally has in all surface magnetic surveys. When the probe passes inside the source body in the on-hole configuration, the orientation of the magnetic field relative to the sensor changes polarity. This property causes a sharp change in the TMI response. The strength of this type of feature depends on the magnetic contrast between adjacent lithologic units. Off-hole magnetic sources, like normal airborne TMI surveys, produce smoothly varying TMI signals (Levanto 1959, 1963) (see Fig. 1 of Ugalde et al. 2007c).

The TMI response of borehole LB-07A varies from approximately –2000 nT to a high of +1000 nT (Fig. 3). The upper part of the log from 330 to 390 m is typified by a reduced TMI response. This is in perfect agreement with the core-based magnetic susceptibility log. The low susceptibility zone from 415 to 470 is approximately equivalent to the monomict lithic breccia zone that is associated with a slight increase in TMI response.

The calculated TMI response for borehole LB-08A is quite different from that observed in borehole LB-07A (Fig. 4). The overall amplitude and frequency response of the TMI signal is similar, but the LB-08A log contains two features not present in the LB-07A log. First, the log shows a sharp drop in amplitude at approximately 290 m. Second, between 290 m and the bottom of the hole (450 m) the TMI gradually increases, reaches a peak of around 1500 nT, and then begins to diminish. These features are characteristic of a situation where the borehole has intersected a strong magnetic contrast (sharp edge) and then is affected by the presence of an off-hole magnetic source (broad high in magnetic response).

DISCUSSION

Because of the differences in sampling rate and source-sensor separation, those magnetic sources that produce localized borehole TMI anomalies of less than 10 m in wavelength will have no consequences for the observed airborne magnetic signal.

Further explanation of the observed TMI response was investigated through a simple forward magnetic model using the Potent magnetic inversion package (Geophysical

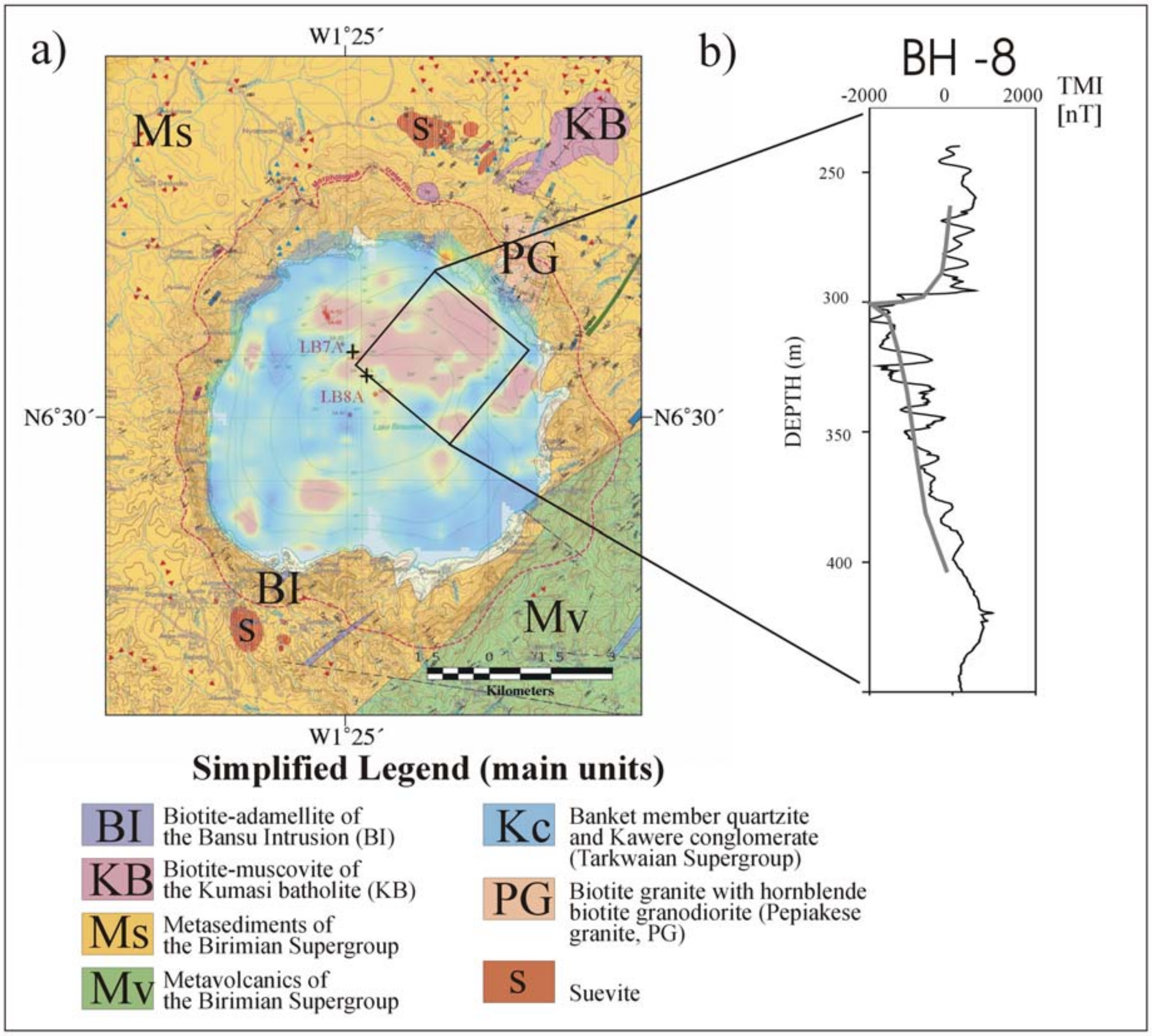

Fig. 5. a) A geological map (after Koeberl and Reimold 2005) overlain with the amplitude of the analytical signal from the marine magnetic data showing close association between magnetic anomalies and basement intrusives. Location of prismatic body calculated on the basis of observed borehole TMI anomaly in borehole LB-08A is indicated by a square. b) Depth section of the model calculated in (a). The model is a prismatic body, with its top at a depth of 300 m and a size of 3000 × 3000 × 3000 m. The borehole barely touches the slab at 300 m, and then does not intersect it anymore. See text for details.

Software Solutions). The form of the TMI response can be replicated by placing a prismatic magnetic source body of 3000 × 3000 × 3000 m, top at 300 m depth, strike = 40°, dip = 15°, k = 0.2 SI to the northwest of the borehole. With a vertical borehole and an inclined source contact, the sharp magnetic boundary is replicated by the borehole passing through an edge of the source body (Fig. 5a). The amplitude of the borehole TMI signal requires that the source body has a strong magnetic contrast compared to surrounding lithologies. However, this can be accomplished by combining high susceptibility with high remanence. A Koenigsberger ratio of 10 and a magnetic susceptibility of 0.018 SI would yield the required effective susceptibility of 0.2. These values are in agreement with the magnetization parameters required by the 3-D model of the magnetic data (Ugalde et al. 2007b), and by those measured in some selected core samples by Kontny et al. (2007). This borehole model is in complete agreement with the observed magnetic data in the lake, as it places the proposed source body over an area of enhanced surface magnetic response (Fig. 5b). As proposed in our companion magnetic modeling paper (Ugalde et al. 2007b), this is quite probably related to granodiorites of the Kumasi batholith, which outcrop to the northeast of the lake, and/or the Bansu intrusion, which outcrops to the southwest (Koeberl and Reimold 2005).

CONCLUSIONS

The results of this study of rock properties from boreholes LB-07A and LB-8A have ramifications for the geophysical models proposed for the Bosumtwi meteorite impact structure (Plado et al 2000; Ugalde et al. 2007a, 2007b).

a. There is no evidence for any on-hole or off-hole strongly magnetic impact-melt mass within the sequence of impact-derived crater fill. Rather the susceptibility data suggest a simple three-layer model comprising upper polymict lithic impact breccia and suevite, monomict lithic impact breccia, and basement rocks (consistent with the lithostratigraphic work by Coney et al. 2007 and Ferrière et al. 2007).
b. Density contrasts are low. Reduced density in the upper part of the basement at borehole LB-08A suggests fracture-induced density reduction is greatest at this location. Density comparisons between LB-07A and LB-08A indicate that there are significant spatial variations in the density of the basement rocks.
c. The borehole total gamma survey shows no evidence of the high radiogenic potassium anomaly that has been described from the airborne survey data (Pesonen et al. 2003).
d. Borehole TMI data derived from the borehole deviation surveys are distinctly different between the two boreholes. LB-07A contains no evidence of any large-scale magnetic sources. LB-08A, in contrast, suggests the presence of a strong magnetic source located in the basement rocks.

Acknowledgments–Drilling at Bosumtwi was supported by the International Continental Scientific Drilling Program (ICDP), the U.S. NSF-Earth System History Program under grant no. ATM-0402010, Austrian FWF (project P17194-N10), the Austrian Academy of Sciences, and by the Canadian Natural Sciences and Engineering Research Council (NSERC). Drilling operations were performed by DOSECC. This research was made possible through the financial support from a NSERC SRO to Bernd Milkereit of the University of Toronto. Jochen Kueck of ICDP (GFZ Potsdam) and his colleagues were of immense help during the collection of this data. We thank the reviewers M. Pilkington and P. Janle, and the associate editor W. U. Reimold, whose input improved the original manuscript.

Editorial Handling—Dr. Wolf Uwe Reimold

REFERENCES

Boamah D. and Koeberl C. 2003. Geology and geochemistry of shallow drill cores from the Bosumtwi impact structure, Ghana. *Meteoritics & Planetary Science* 38:1137–1159.

Chao E. C. T. 1968. Pressure and temperature histories of impact metamorphosed rocks—Based on petrographic observations. In *Shock metamorphism of natural materials*, edited by French B. M. and Short N. M. Baltimore: Mono Book Corp. pp. 135–158.

Cisowski S. M. and Fuller M. 1978. The effect of shock on the magnetism of terrestrial rocks. *Journal of Geophysical Research* 83:3441–3458.

Coney L., Gibson R. L., Reimold W. U., and Koeberl C. 2007. Lithostratigraphic and petrographic analysis of ICDP drill core LB-07A, Bosumtwi impact structure, Ghana. *Meteoritics & Planetary Science* 42. This issue.

Dence M. R., Innes M. J. S., and Beals C. S. 1965. On the probable meteorite origin of the Clearwater Lakes, Quebec. *Journal of the Royal Astronomical Society of Canada* 59:13–22.

Dence M. R. and Popelar J. 1972. Evidence for an impact origin for Lake Wanapitei, Ontario. Geological Association of Canada, Special Paper #10. St. John's, Canada: Geological Association of Canada. pp. 117–124.

Elbra T. and Pesonen L. J. 2006. The Bosumtwi impact structure: Petrophysical, paleomagnetic, and rock magnetic investigations of impactites from BCDP-7A and BCDP-8A deep drill cores (abstract #1578). 37th Lunar and Planetary Science Conference. CD-ROM.

Elbra T., Kontny A., Pesonen L. J., Schleifer N., and Schell C. 2007. Petrophysical and paleomagnetic data of drill cores from the Bosumtwi impact structure, Ghana. *Meteoritics & Planetary Science* 42. This issue.

Ferrière L., Koeberl C., and Reimold W. U. 2007. Drill core LB-08A, Bosumtwi impact structure, Ghana: Petrographic and shock metamorphic studies of rocks from the central uplift. *Meteoritics & Planetary Science* 42. This issue.

Hearst R. B. and Morris W. A. 1995. Rock magnetic properties, why bother? In *Society of Exploration Geophysics Annual Meeting Expanded Technical Program Abstracts with Biographies.* pp. 274–277.

Henkel H. and Reimold W. U. 2002. Magnetic model of the central uplift of the Vredefort impact structure, South Africa. *Journal of Applied Geophysics* 51:43–62.

Koeberl C. and Reimold W. U. 2005 Bosumtwi impact crater, Ghana (West Africa): An updated and revised geological map, with explanations. *Jahrbuch der Geologischen Bundesanstalt, Wien (Yearbook of the Austrian Geological Survey)* 145:31–70 (+1 map, 1:50,000).

Koeberl C., Milkereit B., Overpeck J. T., Scholz C. A., Amoako P. Y. O., Boamah D., Danuor S., Karp T., Kueck J., Hecky R. E., King J. W., and Peck J. A. 2007. An international and multidisciplinary drilling project into a young complex impact structure: The 2004 ICDP Bosumtwi Crater Drilling Project—An overview. *Meteoritics & Planetary Science* 42. This issue.

Kontny A., Elbra T., Just J., Pesonen L. J., Schleicher A. M., and Zolk J. 2007. Petrography and shock-related remagnetization of pyrrhotite in drill cores from the Bosumtwi Impact Crater Drilling Project, Ghana. *Meteoritics & Planetary Science* 42. This issue.

Levanto A. E. 1959. A three component magnetometer for small drillholes and its use in ore prospecting. *Geophysical Prospecting* 7:183–193.

Levanto A. E. 1963. On magnetic measurements on drillholes. *Geoexploration* 2:8–20.

Milkereit B., Ugalde H., Karp T., Scholz C. A., Schmitt D., Danuor S. K., Artemieva N., Kuek J., Qian W., and L'Heureux E. 2006. Exploring the Lake Bosumtwi crater—Geophysical surveys, predictions and drilling results (abstract #1687). 37th Lunar and Planetary Science Conference. CD-ROM.

Pesonen L. J., Koeberl C., and Hautaniemi H. 2003. Airborne geophysical survey of the Lake Bosumtwi impact structure (southern Ghana)—Geophysical maps with descriptions. *Jahrbuch der Geologischen Bundesanstalt, Vienna (Yearbook of the Austrian Geological Society)* 143:581–604.

Pilkington M. and Grieve R. A. F. 1992. The geophysical signature of terrestrial impact craters. *Reviews of Geophysics* 30:161–181.

Plado J., Pesonen L. J., Koeberl C., and Elo S. 2000. The Bosumtwi meteorite impact structure, Ghana: A magnetic model. *Meteoritics & Planetary Science* 35:723–732.

Ugalde H. A., Artemieva N., and Milkereit B. 2005. Magnetization on impact structures—Constraints from numerical modeling and petrophysics. In *Large meteorite impacts III*, edited by Kenkmann T., Hoerz F., and Deutsch A. GSA Special Paper #384. Boulder, Colorado: Geological Society of America. pp. 25–42.

Ugalde H. 2006. Geophysical signature of midsize to small terrestrial impact craters. Ph.D. thesis. University of Toronto, Toronto, Ontario, Canada.

Ugalde H., Danuor S. K., and Milkereit B. 2007a. Integrated 3-D model from gravity and petrophysical data at the Bosumtwi, impact structure, Ghana. *Meteoritics & Planetary Science* 42. This issue.

Ugalde H., Morris W. A., Pesonen L. J., and Danuor S. K. 2007b. The Lake Bosumtwi meteorite impact structure, Ghana—Where is the magnetic source? *Meteoritics & Planetary Science* 42. This issue.

Ugalde H., Morris W. A., Clark C., Miles B., and Milkereit B. 2007c. The Lake Bosumtwi meteorite impact structure, Ghana—A magnetic image from a third observational level. *Meteoritics & Planetary Science* 42. This issue.